Late Pennsylvanian Calcareous Paleosols from Central New Mexico: Implications for Paleoclimate

Spencer G. Lucas and Lawrence H. Tanner

New Mexico Geology, v. 43, n. 1 pp. 3-9, Online ISSN: 2837-6420.
https://doi.org/10.58799/NMG-v43n1.3

This page is intentionally left blank to maintain order of facing pages.

Late Pennsylvanian Calcareous Paleosols from Central New Mexico: Implications for Paleoclimate

Spencer G. Lucas, New Mexico Museum of Natural History and Science, Albuquerque, NM 87104, spencer.lucas@state.nm.us
Lawrence H. Tanner, Department of Biological Sciences, Le Moyne College, Syracuse, NY 13214, tannerlh@lemoyne.edu

Abstract

We document calcareous paleosols from Upper Pennsylvanian (lower Virgilian) strata of the Burrego Member of the Atrasado Formation in the Cerros de Amado of Socorro County, New Mexico. The Burrego paleosols are an excellent example of a scarce, climate-sensitive lithology in the Pennsylvanian strata of New Mexico. These paleosols contain mostly stage II to III carbonate horizons, and their overall morphology suggests deposition and pedogenesis under subhumid, seasonally dry conditions. This conclusion is consistent with paleobotanical and other data that indicate such climate conditions were widespread on Late Pennsylvanian Pangea. The mean value of the oxygen-isotope ratios from Burrego paleosol carbonates compares well with the values from Virgilian paleosols of the San Juan, the eastern Midland and Chama basins of New Mexico-Texas, suggesting similar conditions of temperature and paleoprecipitation. Application of the diffusion-reaction model to the mean carbon-isotope composition of the carbonate suggests a paleo-pCO_2 of approximately 400 ppmV, which is also consistent with estimates from correlative carbonate deposits that formed farther east in Late Pennsylvanian Pangea.

Introduction

What have been called "climate-sensitive lithologies" are rock types specific to a particular climate, the best known being coal (wet), gypsum (dry) and calcareous paleosols (seasonally wet/dry). Such rock types play a prominent role in the interpretation of past climates, constrain climate models and are critical to paleogeographic reconstructions (e.g., Boucot et al., 2013; Cao et al., 2019). However, the distribution of climate-sensitive lithologies remains unevenly and incompletely documented, particularly in older geological time periods.

Indeed, in the Pennsylvanian sedimentary rocks of New Mexico, relatively few such rocks have been documented. Thus, coal beds are few and mostly thin, localized and confined to early Middle Pennsylvanian (Atokan) strata (e.g., Armstrong et al., 1979; Kues and Giles, 2004; Krainer and Lucas, 2013). Gypsum beds are rare, with one well documented example in early Late Pennsylvanian (Missourian) strata (Rejas, 1965; Lucas et al., 2009; Falcon-Lang et al., 2011). Paleosols of Pennyslvanian age, especially climate-sensitive calcareous paleosols, have only been documented from two late Paleozoic basins in northern New Mexico (Tabor et al., 2008; Tanner and Lucas, 2017, 2018). Here, we add to this sparse record of climate-sensitive rocks in the New Mexican Pennsylvanian strata a succession of calcareous paleosols in lower Virgilian strata of Socorro County (Fig. 1).

Stratigraphic context

The calcareous paleosols documented here are in the Burrego Member of the Atrasado Formation, strata that encompass the Missourian-Virgilian boundary, in the Cerros de Amado of Socorro County (Figs. 1-2). Thompson

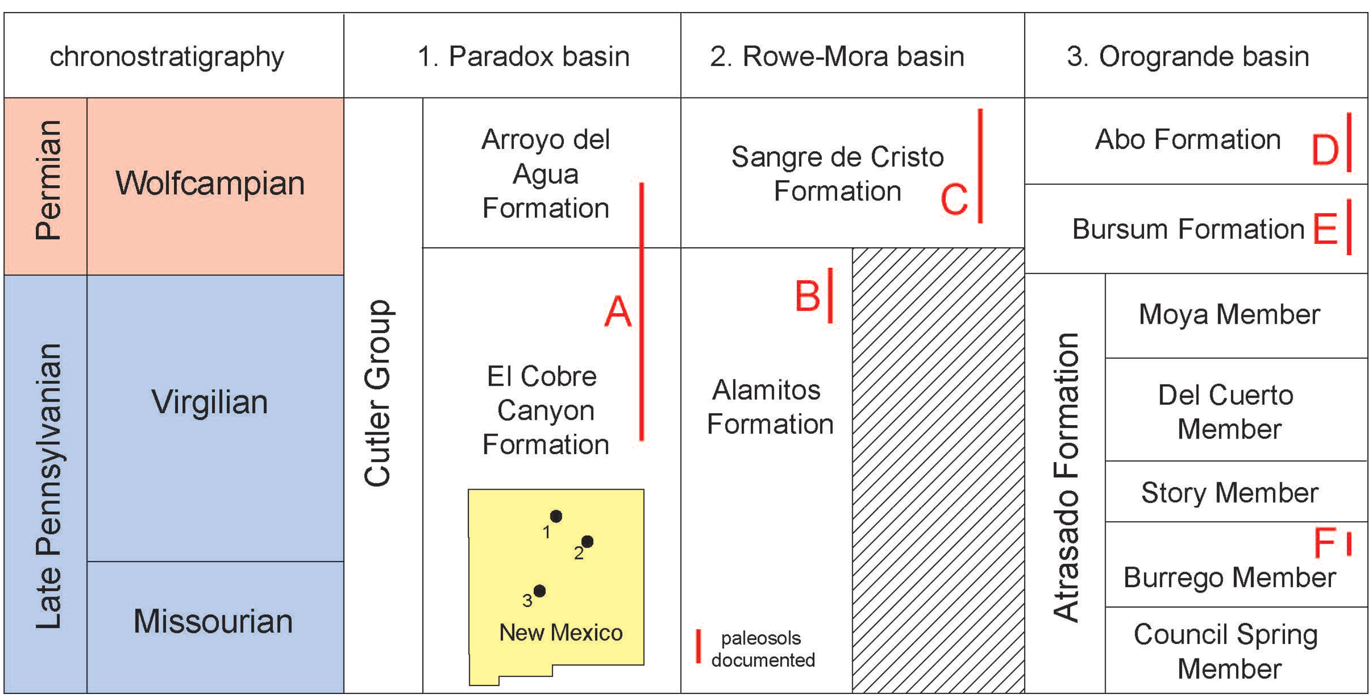

Figure 1. Three late Paleozoic basins in New Mexico that have documented calcareous paleosols of Late Pennsylvanian-early Permian age. Relevant publications are A = Tanner and Lucas (2018); B= Tabor et al. (2008); C = Tanner and Lucas (2017); D = Mack (2003) and references cited therein; E = Tabor et al. (2008); F = this paper.

(1942) presented the first detailed lithostratigraphy and biostratigraphy of the Middle-Upper Pennsylvanian strata that crop out in central and southern New Mexico. In this monograph, Thompson (1942) named six formation-rank units in the northern Oscura Mountains of Socorro County that Lucas and Krainer (2009) reduced in rank to members of the Atrasado Formation, including the Burrego Member.

Rejas (1965), in an unpublished master's thesis, brought much of Thompson's (1942) stratigraphic nomenclature into the Cerros de Amado region east of Socorro (also see Kottlowski, 1960). He used Burrego Member much as did Thompson (1942), as a slope forming, mixed clastic-carbonate interval between two prominent limestone units, the Council Spring Member (below) and Story Member (above).

Lucas et al. (2009), Barrick et al. (2013) and Krainer et al. (2017) published stratigraphic sections of the Burrego Member and adjacent strata at several locations in the Cerros de Amado and vicinity. However, the section described here, though very close to one of the sections Lucas et al. (2009) published (their Minas de Chupadera section) was not studied by them. We discovered this section during fieldwork in 2018.

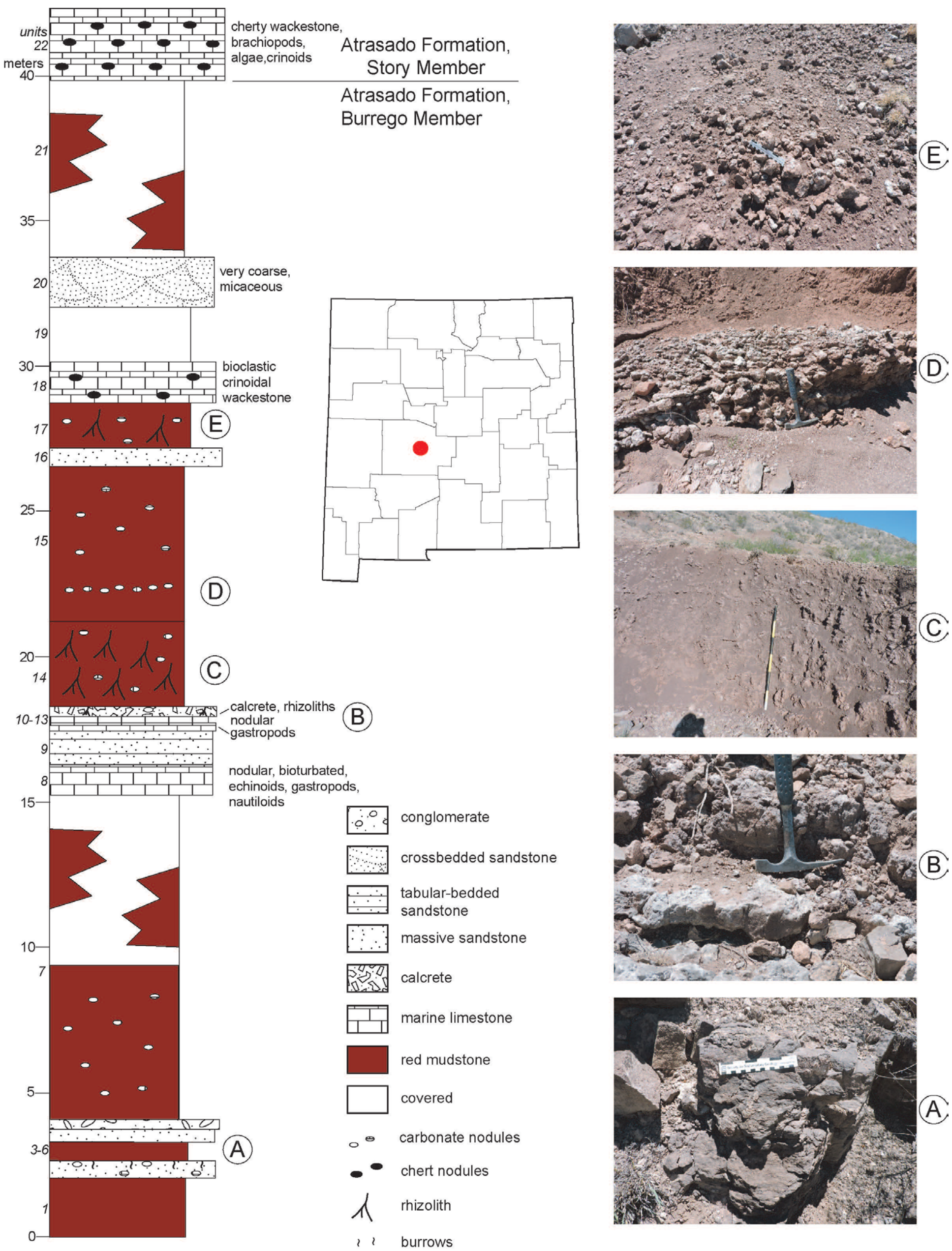

Figure 2. Stratigraphic section of the Burrego Member of the Atrasado Formation near Minas de Chupadera in Socorro County (base of section at UTM 333433, 3775122 and top at 333299, 3775300, zone 13, datum NAD 83; inset map of New Mexico shows location of section in Socorro County). On left, lithostratigraphy of the measured section with the calcareous paleosols in the section labeled A–E. On right, field photographs of the calcareous paleosols A–E.

In the Cerros de Amado, the Burrego Member is 13–55 m thick and consists mostly of slope-forming mudstone and shale interbedded with arkosic/micaceous sandstone and limestone (Rejas, 1965; Lucas et al., 2009; Barrick et al., 2013; Krainer et al., 2017). Most limestone beds in the Burrego Member are evidently of marine origin, as they contain marine macrofossils, including algae, crinoids, molluscs and brachiopods. Conodont and fusulinid biostratigraphy indicates the Borrego paleosols are close in age to the Missourian–Virgilian boundary, and we consider them here to be of early Virgilian age (Lucas et al., 2009; Barrick et al., 2013).

Material and methods

We used standard field methods with a 1.5-m staff, tape measure and Brunton pocket transit to measure the thickness of strata in the stratigraphic section discussed here, which is located in the SE ¼ sec. 26, T2S, R1E (UTM coordinates are in the caption to Figure 2), (Fig. 2). Samples were collected for petrographic and isotopic analysis. To confirm the pedogenic origin of the carbonate, standard 30 µm petrographic thin sections were examined for pedogenic fabrics and textures and for evidence of diagenetic effects.

Carbonate aliquots for isotopic analysis were obtained by selectively drilling micritic calcite in lapped slabs corresponding to prepared thin sections with an ultrafine engraving tool while viewing under a binocular microscope. The samples were analyzed for $\delta^{18}O$ and $\delta^{13}C$ by the Duke Environmental Stable Isotope Laboratory (Nicholas School of the Environment, Duke University, Durham, North Carolina) using standard operating procedures (see Tanner and Lucas, 2018, for details).

We calculated paleo-pCO_2 using the mean $\delta^{13}C$ value from 8 samples and the diffusion-reaction model of Cerling (1991, 1999). But, as we did not obtain organic matter from the samples for determination of $\delta^{13}C_{om}$, we applied values from the literature for formations of similar age and geographic proximity (within 2 degrees latitude), primarily from the published data supplements to Montañez et al. (2007, 2016).

Outcrop description

Where the paleosols in the section display sufficiently distinctive pedogenic features to allow classification, we apply the terminology of Mack et al. (1993) in assigning names of paleosol orders, modified by adjectives describing the most prominent subordinate characteristic. The most common paleosol types we found in the measured section are calcic Argillisols and Calcisols to argillic Calcisols. The calcic Argillisol denotes a paleosol horizon in which the defining characteristic is a clay-rich B horizon that is visibly enriched in $CaCO_3$ in the form of nodules, i.e., a Btk horizon. In any paleosol profile with multiple defining characteristics, such as illuviated clays and pedogenic carbonate, whether they occur in the same horizon or in separate horizons, a subjective judgement was made to determine which feature is dominant and which is subordinate. Thus, there may be a fine distinction between a calcic Argillisol and an argillic Calcisol. In profiles where development of the calcareous B horizons (Bk, or Btk if argillic and calcic) is stronger than the argillic (Bt) horizons, we assign the designation Calcisol or argillic Calcisol, as appropriate. In addition to Argillisols and Calcisols, and variations thereof, we recognize calcic Vertisols, paleosols with prominent vertic fractures and calcareous features in the B horizon. Many mudstone beds of varying thickness display pedogenic features, such as calcareous nodules, drab colors and root traces, but lack distinct horizonation. We term these units Protosols, and where they contain calcareous nodules we label them calcic Protosols. Most paleosol profiles in the section are truncated in that they lack a discernible eluviated upper (A) horizon and display evidence of sediment removal. We also recognize compound profiles in the section. These are marked by repetition of specific types of B horizons (Bt, Btk or Bk) without an intervening A horizon, suggesting an erosional episode (Kraus and Hasiotis, 2006).

The stratigraphic section we measured encompasses ~ 40 m of most of the Burrego Member and its upper contact with the overlying Story Member (Fig. 2). Most of this stratigraphic section is mudrock, about 82% of the thickness of the strata measured. Minor lithologies are sandstone/conglomerate (11% of the section) and limestone (7% of the section).

The section (Fig. 2) begins with redbed mudstone overlain by a thin-bedded, ripple-laminated, very-fine grained sandstone that is 0.5 m thick (units 2–3). This sandstone has a platy fabric and contains some discrete calcareous nodules and scarce root traces that increase in abundance upward and has a bioturbated/pedoturbated top. The top 0.1 m is a well-developed carbonate horizon (Stage II of Gile et al., 1966) with carbonate nodules 1 to 2 cm in diameter, drab root traces and rhizoliths up to 5 cm long. We consider unit 2 a truncated Calcisol that is relatively immature, given the lack of coalescing nodules, consisting only of C and Bk horizons. It is overlain by 0.3 m of red mudstone (unit 4) followed by a 0.3-m-thick bed of coarse-grained, arkosic sandstone capped by a 0.1-m-thick limestone-pebble conglomerate (units 5–6). Some of the limestone pebbles in this conglomerate contain marine macrofossils, including brachiopods and gastropods. The overlying unit 7 is 11.3 m thick and is a red mudstone slope with its upper half covered by mostly colluvium. The lower half of this unit has numerous carbonate nodules isolated in the mudstone, but lacks distinct horizonation. Therefore, we consider this unit a calcic Protosol.

Above unit 7 is a nodular and bioturbated limestone (unit 8) rich in marine macrofossils, including echinoids, gastropods and nautiloids. A 1.2-m-thick, very coarse-grained, arkosic sandstone bed (unit 9) above has limestone rip-ups at its base and displays somewhat indistinct, tabular bedding. The overlying interval of limestone (units 10–13) begins with a 0.2-m-thick bed of lime mudstone with sparse fossils of marine gastropods, capped by a 0.2 to 0.3-m-thick dark to light limestone bed that is nodular, and the weathered surface has vertical channels up to 2.5 cm wide and 10 cm long that are filled with smaller calcareous nodules. We infer that these record root channels formed during subaerial exposure and pedogenesis of the marine carbonate. The top of the unit is a 0.1 m mudstone/limestone breccia consisting of limestone blocks up to 4 cm in a red mudstone matrix with root traces and small calcareous nodules. This unit represents a calcic Argillisol formed on the reworked limestone surface.

Unit 14 is 2.9 m of dark brown, fine-grained mudstone with a crumb fabric, but the outstanding feature of the unit is the presence of numerous rhizoliths. These are calcareous masses that weather out of the outcrop face, mostly vertically oriented and irregular (noncylindrical) in shape. The masses are up to 1.0 m long, 0.1 m in diameter and have no internal structure. Most of these features have a rough, knobby appearance because they consist of vertically stacked, calcareous oblate spheroids of varying diameters. Many of them taper downward, and some exhibit branching, supporting their interpretation as rhizoliths. The unit also contains subhorizontal arcuate soil fractures and irregular (botryoidal) calcareous masses up to 0.1 m wide. Unit 14 lacks any horizonation, so it is interpreted to represent a single B horizon containing calcareous nodules and vertic fractures. We classify this unit as a calcic Vertisol that formed through an extended interval of continuous sedimentation (aggradation) during pedogenesis, in other words, a cumulative paleosol. The outcrop does not contain the top of the unit, and no A-horizon is preserved.

The overlying 5.4 m of red mudstone (unit 15) has clay-lined root traces and numerous carbonate nodules that increase upward to form a coalesced (Stage III to IV) layer 0.6 m thick that is exposed over a lateral extent of 5 m. We regard this unit as the Btk horizon of an argillic Calcisol. The unit is truncated above abruptly by a massive, 0.5-m-thick sandstone ledge (unit 16). The sandstone is overlain by 1.7 m of red mudstone with drab-brown mottling at the top (unit 17). The mudstone contains numerous rhizoliths and calcareous nodules that increase in abundance vertically to form two horizons, each approximately 0.3 m thick, of carbonate nodules up to 8 cm in diameter, which coalesce to form Stage II to III pedogenic carbonate horizons. Nodules decrease in abundance in the upper 0.4 m of the overlying mudstone interval of unit 17. The transitional nature of the underlying and overlying mudstone intervals of unit 17 suggests that this unit represents a calcareous paleosol, specifically a compound argillic Calcisol with Btk (Stage II) and Bk (Stage III) carbonate horizons.

The overlying bed of limestone (unit 18) is a 1.3 m thick, thickly bedded, cherty bioclastic wackestone with abundant crinoidal debris. Above that is a covered slope 2.1 m thick overlain by a very coarse grained, micaceous, trough crossbedded sandstone (unit 20) that is 1.7 m thick. The uppermost part of the Burrego Member is a 6.1 m thick slope, mostly covered, but where bedrock is exposed on this slope it is red mudstone (unit 21). The base of the overlying Story Member is a medium-bedded, cherty wackestone with fossils of algae, crinoids and brachiopods.

Outcrop interpretation

As noted above, the Burrego Member is a lithosome that includes a mixture of sediments of marine and nonmarine origin, and the section we studied is representative of that. Thus, limestone beds in the section with marine invertebrate fossils (units 8, 12 and 18) are obviously of marine origin, whereas the other strata are of nonmarine origin.

The relatively thick intervals of red mudstone that host the calcareous paleosols we studied are readily interpreted as nonmarine deposits of alluvial floodplains that have undergone variable amounts of pedogenesis. Sandstones in the section are likely of fluvial origin, and limestone clasts in the conglomerate low in the section (unit 6) contain marine invertebrate fossils, which suggests proximity to marine carbonate beds. Thus, we interpret the section as mostly representing floodplain deposition close to the shoreline and sea, interrupted by marine incursions.

The section we studied includes meter-scale profiles of simple and cumulative paleosols, including calcic Argillisols, argillic Calcisols, Calcisols and calcic Vertisols. Most samples for isotopic analysis were selected from argillic Calcisols and Calcisols with well-developed (Stage III to Stage IV *sensu* Gile et al., 1966; Machette, 1985) carbonate horizons hosted in argillic red beds. Examination of petrographic thin sections indicates that pedogenic carbonate in the section consists of micritic calcite with displacive textures and fabrics, including circumgranular cracking, that demonstrate a lack of diagenetic replacement (Fig. 3). Samples generally were selected from below the coalesced carbonate horizon to maximize depth below the original soil surface.

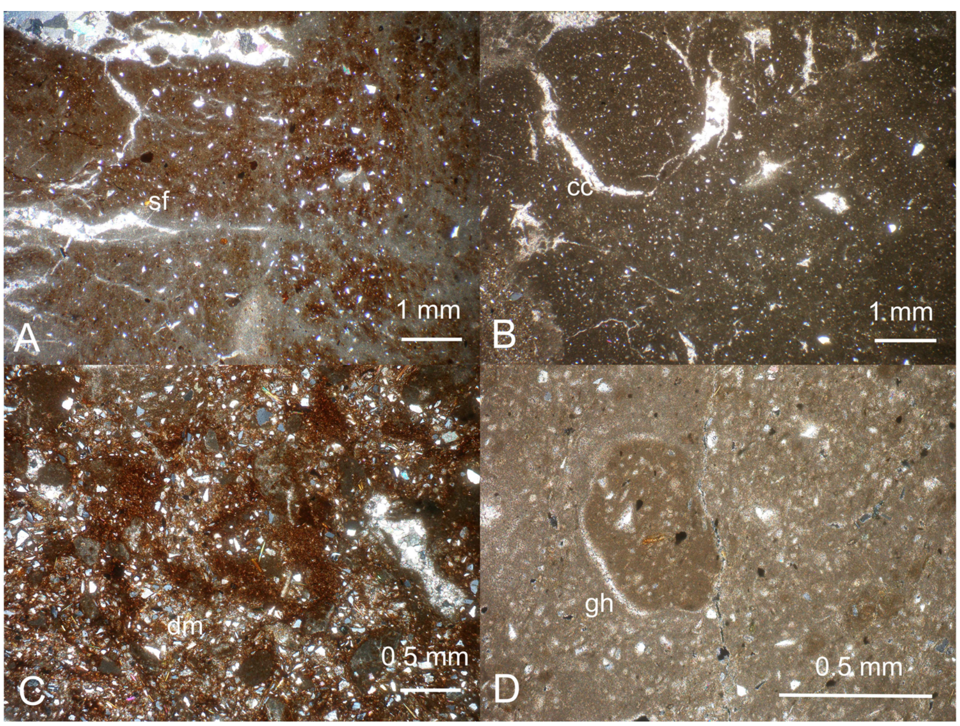

Figure 3. Petrographic features of Burrego Member calcic paleosols. A) Spar-filled voids and shrinkage fractures (sf). B) Mudstone clast surrounded by circumgranular crack (cc). C) Mudstone matrix with displacive micrite (dm). D) Mudstone clast surrounded by sparry grain halo (gh).

Paleosol analysis

Four paleosols were sampled for isotopic analysis (labelled A, C, D and E in Figure 2). In ascending order these are: (1) a thin Calcisol with Stage II calcareous paleosol developed in a blocky, very-fine grained sandstone containing calcareous rhizoliths (station A); station B is a nodular carbonate formed on a marine limestone and was not sampled due to the likelihood of incorporation of marine carbonate; (2) station C is a calcic Vertisol exposure, 2.9-m thick, notable for the abundance of calcite-cemented rhizoliths up to 1 meter in vertical length in a mudstone matrix with blocky ped fabric; (3) station D is a Calcisol with a prominent Stage III nodular horizon; and (4) station E is a calcic Argillisol containing two nodular horizons exhibiting Stage II and Stage III morphology, likely representing stages in formation of a cumulative soil.

Petrography reveals the presence of typical alpha-type fabrics in the carbonate nodules sampled in the section, such as grain coronas and corroded floating grains that indicate that these nodules represent the accumulation of carbonate in the B horizon of paleosols (Fig. 3; Alonso-Zarza and Wright, 2010). Thus, we are confident that these carbonates formed within soils developed on alluvial muds.

Isotopic analysis of eight carbonate samples from the Burrego Member are tightly clustered and yielded $\delta^{13}C_{carb}$ values ranging from -6.4 ‰ to -5.6 ‰ with a mean of -6.0 ± 0.1 ‰ (VPDB) (Table 1). The isotopic composition of two samples from rhizoliths at Station C (-6.0 ‰, -5.6 ‰ (VPDB)) is the same as measured in samples of carbonate nodules, suggesting micritization of the root casts in the deep (>50 cm depth) soil environment and therefore representative of the isotopic composition of soil respired CO_2. Values of $\delta^{18}O$ have a wider spread, ranging from -5.7 to -1.8 ‰, with a mean value of -3.4 + 0.5‰ (VPDB). The greater range for $\delta^{18}O$ likely records pedogenic carbonate precipitation under a range of temperature and/or precipitation conditions. The composition of the carbonate is determined by a combination of factors in the diffusion model: plant respiration rate, isotopic composition of the plant organic matter (OM), atmospheric isotope composition and pCO_2. The isotopic composition of the plant OM tells us about the vegetation, but only in the most general sense (C3 vs C4), and nothing is known about any possibly unique isotopic aspects of Pennsylvanian plant OM.

The lack of $\delta^{13}C_{om}$ measurements in this study makes application of the diffusion-reaction model of Cerling (1991; 1999) somewhat problematic. However, the datasets of Montañez et al. (2007, 2016) provide useful measurements of $\delta^{13}C_{om}$ that allow us to at least make an approximation of paleo-pCO_2. Temperature of soil carbonate formation, the isotopic composition of atmospheric CO_2 and the contribution of soil-respired CO_2 (the S(z) term) are also required for application of the model. We assumed values based on (but not identical to) those of Montañez et al. (2007, 2016), using values $\delta^{13}C_{om}$ = -21.0 ‰, $\delta^{13}C_a$ = -2.5 ‰ (composition of atmospheric CO_2), T = 25°C and S(z) = 3000 ppmV. The S(z) value reflects the fact that carbonate precipitation mainly occurs during the drier months when plant productivity is decreased (Breecker, 2013). The Borrego carbonates yielded a mean $\delta^{13}C_{carb}$ of -6.0 ‰. Using the values cited above we obtained a paleo-pCO_2 for the early Virgilian of ~ 400 ppmV. This estimate accords well with values presented by Montañez et al. (2016) for the late Missourian, and the early Virgilian (Fig. 4). The mean $\delta^{18}O$ value of -3.4 $\pm$ 0.5 ‰ (VPDB) obtained compares well with the values from the Virgilian paleosols of the Chama Basin of northern New Mexico (Tanner and Lucas, 2018), suggesting similar conditions of temperature and paleoprecipitation.

Overall, the morphology of the paleosols in the Burrego Member suggests deposition and pedogenesis under subhumid, seasonally dry conditions. The calcareous paleosol horizons vary in maturity from Stage II to IV, and both cumulate and composite paleosol profiles are present, suggesting higher rates of sedimentation during some intervals, alternating with slow sedimentation during others (e.g., Deutz et al., 2002; Monger et al., 2009). In particular, the "mega-rhizolith" horizon at Station C appears to be a single, undifferentiated B horizon with an exposed thickness of 2.9 m. This attests to continuous aggradation of the surface contemporaneous with pedogenic processes, particularly root turbation. The interplay of sedimentation and biological activity with pedogenesis suggests meteoric precipitation at the higher end of the range for which calcareous paleosol formation is considered possible (Birkeland, 1999; Retallack, 2005). Thus, paleosol morphology supports the isotopic analyses in suggesting sediment deposition and soil formation under widely varying moisture conditions.

Table 1. Isotopic analyses of Burrego calcareous paleosol samples. Values in units ‰ VPDB.

Unit	$\delta^{18}O$	$\delta^{13}C$
Station A	-3.8	-5.8
Station C-1	-3.5	-5.6
Station C-2	-4.0	-6.0
Station D-1	-2.6	-6.2
Station D-2A	-4.0	-6.1
Station D-2B	-5.7	-6.4
Station E-1	-1.8	5.9
Station E-2	-2.1	-5.6

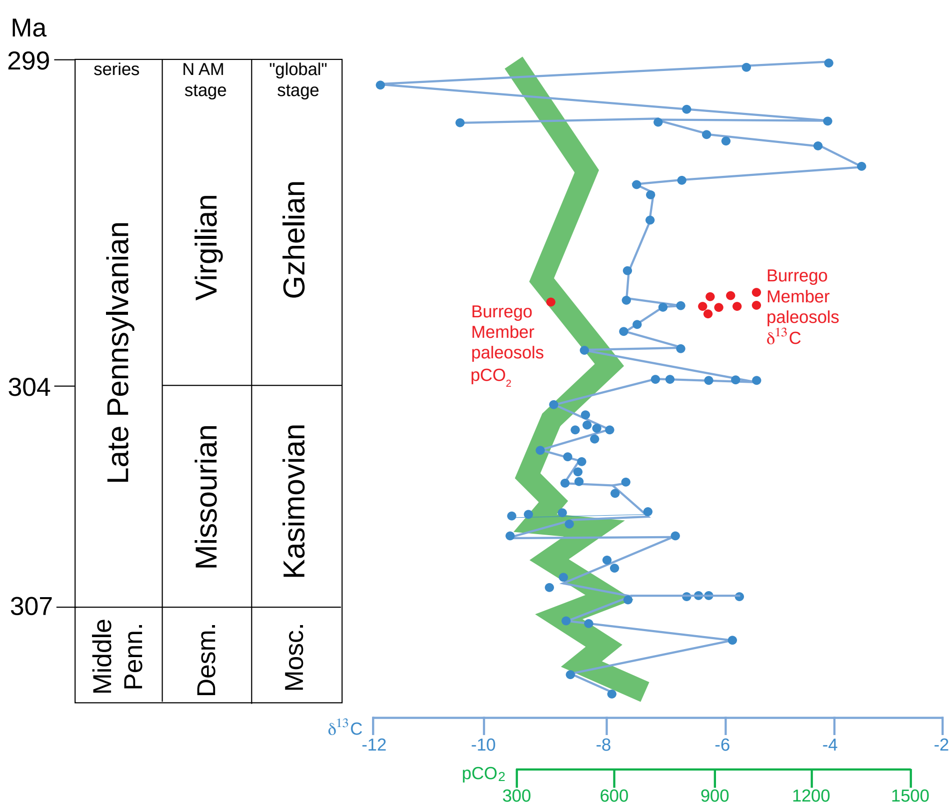

Figure 4. Compilation of Late Pennsylvanian $\delta^{13}C_{carb}$ data from Montañez et al. (2016), the pCO_2 curve of Chen et al. (2018) calculated from the Montañez et al. data, $\delta^{13}C_{carb}$ values obtained in this study, and the calculated pCO_2 value from the Burrego Member.

Discussion

In New Mexico, sedimentary rocks of late Paleozoic age are synorogenic deposits of the Ancestral Rocky Mountain (ARM) orogeny. Driven by the Gondwana–Laurussia collision that amalgamated late Paleozoic–Mesozoic Pangea (e. g., Kluth and Coney, 1981; Dickinson and Lawton, 2003), the ARM in New Mexico produced a series of basement-cored uplifts surrounded by sedimentary basins during Middle Pennsylvanian (Atokan)-early Permian (Wolfcampian) time (e.g., Kues and Giles, 2004; Brotherthon et al., 2020). The result was an archipelago of islands (the uplifts) surrounded by shallow-marine sedimentary basins during the Middle–Late Pennsylvanian, followed by mostly nonmarine deposition in these and reconfigured sedimentary basins during the early Permian culmination of the ARM orogeny. Around the fringes and on the flanks of the uplifts, nonmarine fluvial deposition took place in some locations during the Pennsylvanian, such as the section described here, and by early Permian time fluvial deposits (largely siliciclastic red beds) were filling the formerly marine basins.

Calcareous paleosols are comparatively common in lower Permian strata in New Mexico (particularly in the Abo Formation: Mack, 2003 and references cited therein), but a few Virgilian calcareous paleosols are the only Pennsylvanian examples that have been documented prior to the Burrego Member record documented here. Thus, Tabor et al. (2008) briefly discussed a few late Virgilian calcareous paleosols in the Rowe–Mora basin (Taos trough) and in the Bursum Formation of southern New Mexico, and Tanner and Lucas (2018) documented similar late Virgilian paleosols in part of the Paradox basin (Fig. 1). These workers concluded that the Virgilian paleosols indicate highly variable climate ranging from subhumid to semiarid with extremes in seasonal precipitation, which is consistent with our interpretation of the Burrego paleosols.

New Mexico was located near the western end of the Pangean tropical belt during the Late Pennsylvanian. Climate models, paleosol data and paleobotany converge to identify a distinct monsoonal pattern of moisture in western Pangea during the Late Pennsylvanian–early Permian, with moisture sourced from Panthalassa (e.g., Parrish, 1993; Tabor and Montañez, 2004; Tabor and Poulsen, 2008). There was a global shift from wetter Middle Pennsylvanian climates to drier Late Pennsylvanian climates that began in New Mexico during the Middle Pennsylvanian (Desmoinesian) when floras with seasonally dry elements begin to appear and then become more common during the Late Pennsylvanian and early Permian (DiMichele et al., 2011, 2017).

In central New Mexico, the Atrasado Formation, including the Burrego Member, contains a succession of paleofloras that are all of “mixed” composition. This means that plants that favored wet substrates and those from habitats with seasonal moisture limitations are mixed together in the fossil assemblages and evidently grew in close proximity. These floras indicate climates that varied from subhumid to semiarid and arid (DiMichele et al., 2017).

The Burrego paleosols formed in a subhumid climate under seasonally dry conditions. The pCO_2 value of ~ 400 ppm we calculate is within the range of values given by Montañez et al. (2016, fig. 2) across the Missourian–Virgilian boundary. Thus, the Burrego paleosols indicate a climate within the range of what were thought to be the climates of equatorial Pangea during the Late Pennsylvanian—subhumid and seasonally dry. The Burrego paleosols thus add an important data point of climate sensitive lithologies from what was far western, tropical Pangea during the Late Pennsylvanian.

Acknowledgments

The comments of the reviewers, D. O. Breecker and H. C. Monger, and the editor, B. D. Allen, improved the content and clarity of the manuscript.

References

Alonso-Zarza, A.M. and Wright, V.P., 2010b, Calcretes; *in* Alonso-Zarza, A.M. and Tanner, L.H., eds., Carbonates in Continental Environments: Processes, Facies and Applications: Developments in Sedimentology 61: Elsevier, Amsterdam, p. 226–267.

Armstrong, A.K., Kottlowski, F.E., Stewart, W.J., Mamet, B.L., Baltz, E.H., Jr., Siemers, W.T. and Thompson, S., III, 1979. The Mississippian and Pennsylvanian (Carboniferous) systems in the United States—New Mexico. U. S. Geological Survey, Professional Paper 1110-W, p. W1–W27.

Barrick, J., Lucas, S .G., and Krainer, K., 2013, Conodonts of the Atrasado Formation (uppermost Middle to Upper Pennsylvanian), Cerros de Amado region, central New Mexico, USA: New Mexico Museum of Natural History and Science, Bulletin 59, p. 239–252.

Birkeland, P.W., 1999, Soils and Geomorphology, 3rd ed., Oxford, New York, 536 pp.

Boucot, A.J., Chen, X., Scotes, C.R. and Morley, R.J., 2013, Phanerozoic paleoclimate: an atlas of lithologic indicators of climate: SEPM Concepts in Sedimentology and Paleontology, no. 11, Map Folio, 28 maps.

Breecker, D.O., 2013, Quantifying and understanding the uncertainty of atmospheric CO_2 concentrations determined from calcic paleosols: Geochemistry, Geophysics, Geosystems, v. 14, p. 3210–3220.

Brotherton, J.L., Chowdhury, N.U.M.K., and Sweet, D.E., 2020, Synthesis of late Paleozoic sedimentation in central and eastern New Mexico: Implications for timing of ancestral Rocky Mountains deformation: SEPM Special Publication 113. doi: 10.102110/sepmsp.113.03.

Cao, W., Williams, S., Flament, M., Sahirovic, S, Scotese, C. and Müller, R.D., 2019, Palaeolatitudinal distribution of lithologic indicators of climate in a palaeogeographic framework: Geological Magazine, v. 156, p. 331–354.

Cerling, T.E., 1991, Carbon dioxide in the atmosphere: evidence from Cenozoic and Mesozoic paleosols: American Journal of Science, v. 291, p. 377–400.

Cerling, T.E., 1999, Stable carbon isotopes in palaeosol carbonates; *in* Thiry, M. and Simon-Coinçon, R., eds., Palaeoweathering, palaeosurfaces and related continental deposits: International Association of Sedimentologists, Special Publication 27, p. 43–60.

Chen, J., Montañez, I.P., Qi, Y., Shen, S., and Wang, X., 2018, Strontium and carbon isotopic evidence for decoupling of pCO_2 from continental weathering at the apex of the late Paleozoic glaciation: Geology, v. 46, p. 395–398.

Deutz, P., Montañez, I.P. and Monger, H.C., 2002, Morphology and stable and radiogenic isotope composition of pedogenic carbonates in late Quaternary relict soils, New Mexico, USA: an integrated record of pedogenic overprinting: Journal of Sedimentary Research, v. 72, p.809–822.

Dickinson, W.R., and Lawton, T.F., 2003, Sequential intercontinental suturing as the ultimate control of Pennsylvanian Ancestral Rocky Mountains deformation: Geology, v. 31, p. 609–612.

DiMichele, W.D., Cecil, C.B., Chaney, D.S., Elrick, S.D., Lucas, S.G., Lupia, R., Nelson, W.J. and Tabor, N.J., 2011, Pennsylvanian-Permian vegetational changes in tropical Euramerica; *in* Harper, J.A., ed., Geology of the Pennsylvanian-Permian in the Dunkard basin: 76th Annual Field Conference of Pennsylvania Geologists Guidebook, Washington, PA, p. 60–102.

DiMichele, W.A., Chaney, D.S., Lucas, S.G., Nelson, W.J., Elrick, S.D., Falcon-Lang, H.J. and Kerp, H., 2017, Middle and Late Pennsylvanian fossil floras from Socorro County, New Mexico, U.S.A: New Mexico Museum of Natural History and Science, Bulletin 77, p. 25–99.

Falcon-Lang, H.J., Jud, N.A., Nelson, W.J., DiMichele, W.A., Chaney, D.S. and Lucas, S.G., 2011, Pennsylvanian coniferopsid forests in sabkha facies reveal the nature of seasonal tropical biome: Geology, v. 39, p. 371–374.

Gile, L.H., Peterson, F.F., and Grossman, R.B., 1966, Morphological and genetic sequences of accumulation in desert soils: Soil Science, v. 100, p. 347–360.

Kluth, C.F. and Coney, P.J., 1981, Plate tectonics of the Ancestral Rocky Mountains: Geology, v. 9, p. 10–15.

Kottlowski, F.E., 1960, Summary of Pennsylvanian sections in southwestern New Mexico and southeastern Arizona: New Mexico Bureau of Mines and Mineral Resources, Bulletin 66, 187 p.

Krainer, K., and Lucas, S.G., 2013,The Pennsylvanian Sandia Formation in northern and central New Mexico: New Mexico Museum of Natural History and Science, Bulletin 59, p. 77–100.

Krainer, K., Vachard, D., Lucas S.G., and Ernst, A., 2017, Microfacies and sedimentary petrography of Pennsylvanian limestones and sandstones of the Cerros de Amado Area, east of Socorro (New Mexico, USA): New Mexico Museum of Natural History and Science, Bulletin 77, p. 159–198.

Kraus, M.J. and Hasiotis, S.T., 2006, Significance of different modes of rhizolith preservation to interpreting paleoenvironmental and paleohydrologic settings: examples from Paleogene paleosols, Bighorn Basin, Wyoming, U.S.A.: Journal of Sedimentary Research, v. 76, p. 633–646.

Kues B.S., and Giles K.A., 2004, The late Paleozoic Ancestral Rocky Mountains system in New Mexico; *in* Mack G.H., and Giles, K.A., eds., The Geology of New Mexico, A Geologic History: New Mexico Geological Society, Special Publication 11, p. 95–136.

Lucas, S.G. and Krainer, K., 2009, Pennsylvanian stratigraphy in the northern Oscura Mountains, Socorro County, New Mexico: New Mexico Geological Society, Guidebook 60, p. 153–166.

Lucas, S.G., Krainer, K., and Barrick, J.E., 2009, Pennsylvanian stratigraphy and conodont biostratigraphy in the Cerros de Amado, Socorro County, New Mexico: New Mexico Geological Society, Guidebook 60, p. 183–212.

Machette, M.N., 1985, Calcic soils of the southwestern United States: Geological Society of America, Special Paper 203, p. 1–21.

Mack, G.H., 2003, Lower Permian terrestrial palaeoclimate indicators in New Mexico and their comparison to palaeoclimate models: New Mexico Geological Society, Guidebook 54, p. 231–240.

Mack, G.H., James, W.C., and Monger, H.C., 1993, Classification of paleosols: Geological Society of America Bulletin, v. 105, p. 129–136.

Monger, H.C., Cole, D.R., Buck, B.J. and Gallegos, R.A., 2009, Scale and the isotopic record of C4 plants in pedogenic carbonate: from the biome to the rhizosphere: Ecology, v. 90, p.1498–1511.

Montañez, I.P., Tabor, N.J., Niemeier, D., DiMichele, W.A., Frank, T.D., Fielding , C.R., and Isbell, J.L., 2007, CO_2-forced climate and vegetation instability during late Paleozoic deglaciation: Science, v. 315, p. 87–91.

Montañez, I.P., McElwain, J.C., Poulsen, C.J., White, J.D., DiMichele, W.A., Wilson, J.P., Griggs, G., and Hren, M.T., 2016, Climate pCO_2 and terrestrial carbon cycle linkages during Late Palaeozoic glacial-interglacial cycles: Nature Geoscience, v. 9, p. 824–831.

Parrish, J.T., 1993, Climate of the supercontinent Pangaea: Journal of Geology, v. 101, p. 215–33.

Rejas, A., 1965, Geology of the Cerros de Amado area, Socorro County, New Mexico: [M.S. thesis]: New Mexico Institute of Mining and Technology, Socorro, 128 p.

Retallack, G.J., 2005, Pedogenic carbonate proxies for amount and seasonality of precipitation in paleosols: Geology, v. 33, p. 333–336.

Tabor, N.J., and Montañez, I.P., 2004, Permo-Pennsylvanian alluvial paleosols (north-central Texas): High-resolution proxy records of the evolution of early Pangean paleoclimate: Sedimentology, v. 51, p. 851–884.

Tabor, N.J. and Poulsen, C.J., 2008, Palaeoclimate across the Late Pennsylvanian–early Permian tropical palaeolatitudes: a review of climate indicators, their distribution, and relation to palaeophysiographic climate factors: Palaeogeography, Palaeoclimatology, Palaeoecology, v. 268, p. 293–310.

Tabor, N.J., Montañez, I.P., Scotese, C.R., Poulsen, C.J. and Mack, G.H., 2008, Paleosol archives of environmental and climatic history in paleotropical western Pangea during the latest Pennsylvanian through Early Permian: Geological Society of America, Special Paper 441, p. 291–303.

Tanner, L.H., and Lucas, S.G., 2017, Paleosols of the Upper Paleozoic Sangre de Cristo Formation, north-central New Mexico: Record of early Permian palaeoclimate in tropical Pangea: Journal of Palaeogeography, v. 6, p. 144–162.

Tanner, L.H., and Lucas, S.G., 2018, Pedogenic record of climate change across the Pennsylvanian–Permian boundary in red-bed strata of the Cutler Group, northern New Mexico, USA: Sedimentary Geology, v. 373, p. 98–110.

Thompson, M.L., 1942, Pennsylvanian System in New Mexico: New Mexico School of Mines, State Bureau of Mines and Mineral Resources, Bulletin 17, 92 p.